AD-A130 095 A STUDY OF THE ANGULAR RADIATION PATTERN OF SMITH-PURCELL RADIATION(U) TEL-AVIV UNIV (ISRAEL) SCHOOL OF ENGINEERING A GOVER ET AL. 20 MAY 83 1/1

UNCLASSIFIED AFOSR-TR-83-0566 AFOSR-81-0060 F/G 20/7 NL

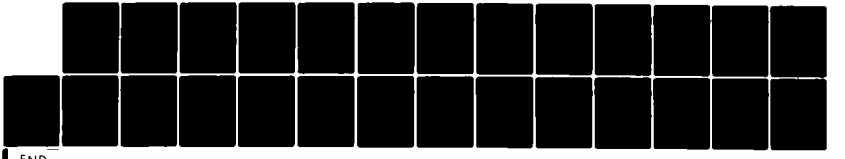

END
DATE FILMED
7-83
DTIC

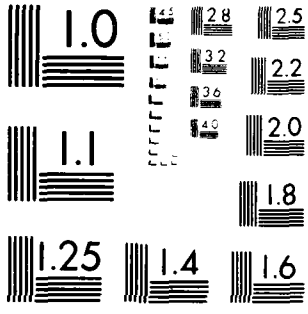

TEL AVIV UNIERSITY FACULTY OF ENGINEERING

Tel-Aviv, Israel

Final Scientific Report Grant No. AFOSR-81-060

Nov. 80 - Oct. 81

# A STUDY OF THE ANGULAR RADIATION PATTERN OF SMITH-PURCELL RADIATION

by

A. Gover, P. Dvorkis and U. Elisha

May 20, 1983

Prepared for the

Air Force Office of Scientific Research and Development,

Bolling AFB, Washington, D. C., U.S.A.

and the

European Office of Aerospace Research and Development,

London, England

UNCLASSIFIED

SECURITY CLASSIFICATION OF THIS PAGE (When Data Entered)

| REPORT DOCUMENTATION PAGE | | READ INSTRUCTIONS BEFORE COMPLETING FORM |
|---|---|---|
| 1. REPORT NUMBER AFOSR-TR- 83-0566 | 2. GOVT ACCESSION NO. | 3. RECIPIENT'S CATALOG NUMBER |
| 4. TITLE (and Subtitle) A Study of the Angular Radiation Pattern of Smith-Purcell Radiation | | 5. TYPE OF REPORT & PERIOD COVERED Final Scientific Report Nov. 80 - Oct. 81 |
| | | 6. PERFORMING ORG. REPORT NUMBER |
| 7. AUTHOR(s) A. Gover, P. Dvorkis, U. Elisha | | 8. CONTRACT OR GRANT NUMBER(s) AFOSR-81-0060 |
| 9. PERFORMING ORGANIZATION NAME AND ADDRESS Tel Aviv University Faculty of Engineering Tel Aviv, Israel | | 10. PROGRAM ELEMENT, PROJECT, TASK AREA & WORK UNIT NUMBERS 2301-A1 61102F |
| 11. CONTROLLING OFFICE NAME AND ADDRESS Air Force Office of Scientific Research/NP Bolling AFB, Washington, D.C. 20332 | | 12. REPORT DATE May 20, 1983 |
| | | 13. NUMBER OF PAGES 26 |
| 14. MONITORING AGENCY NAME & ADDRESS (if different from Controlling Office) European Office of Aerospace Research and Development/NP Box 14, FPO, New York 09510 | | 15. SECURITY CLASS. (of this report) Unclassified |
| | | 15a. DECLASSIFICATION DOWNGRADING SCHEDULE |

16. DISTRIBUTION STATEMENT (of this Report)

Approved for public release, distribution unlimited.

17. DISTRIBUTION STATEMENT (of the abstract entered in Block 20, if different from Report)

18. SUPPLEMENTARY NOTES

19. KEY WORDS (Continue on reverse side if necessary and identify by block number)

Smith-Purcell Radiation, Free Electron Laser, Orotron.

20. ABSTRACT (Continue on reverse side if necessary and identify by block number)

The power radiation pattern of the Smith-Purcell radiation was measured at various latitudes and azimuth angles relative to the electron beam. The experimental data is used to evaluate the various models and physical mechanisms previously suggested to describe the Smith-Purcell radiation. Good agreement was observed between the experimental data and theoretical curves derived from Van-Den-Berg's analysis. The radiation mechanism proposed by Salisbury was analized and shown to be too small to

DD FORM 1 JAN 73 1473 EDITION OF 1 NOV 65 IS OBSOLETE

UNCLASSIFIED

SECURITY CLASSIFICATION OF THIS PAGE (When Data Entered)

20. (cont.) account for the measured radiation. The experiment and Van-Den-Berg's theory perdict stronger emission at azimuthal angles off the plane perpendicular to the gratings. This observation leads to conclusions regarding the design of optical cavities for Smith-Purcell Free Electron Lasers and Orotron milimeter wavelength radiation tube devices.

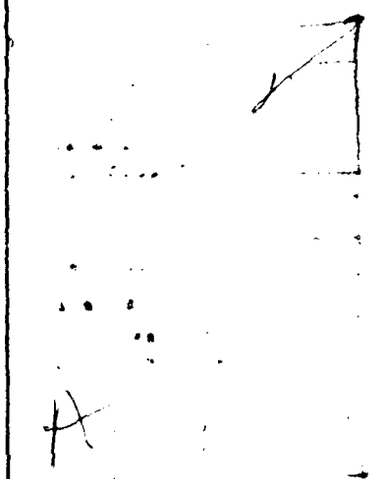

Introduction

We report the results and the interpretation of Smith-Purcell radistion experiments which were carried out in Tel-Aviv Uniersity during the grant period Nov. 80 - Oct. 81 and some time after it.

The experiments were carried out using the electron beam of a Philips EM-300 electron microscope operating at 100, 80 and 60 keV energies and using a variety of optical gratings. We put special emphasis on the quantitative measurement of the radiation power pattern at different angles. This helped to evaluate the validity of various models and physical mechanisms which were suggested before to describe the Smith-Purcell effect. It also helped to draw conclusions on the design of resonator structures for the Smith-Purcell free electron lasers (FEL)[1-3] and for the related milimeter wavelength tube device, the orotron [4-7].

The basic configuration of the Smith-Purcell radiation effect is described in Fig. 1. An electron beam propagates parallel and very closely to the surface of an optical grating, perpendicularly to the grating rulings. At any angle $\eta$ relative to the plane perpendicular to the beam direction (viz. 90°-$\eta$ angle relative to the beam direction) radiation is emitted at a wavelength

$$\lambda_n = -\frac{D}{n}\left(c/v_0 - \sin\eta\right) \qquad (1)$$

where D is the grating period, $v_0$ is the electron velocity and n is a negative integer.

Various models and mechanisms were proposed to explain the experimentally observed effect. Smith and Purcell explained the

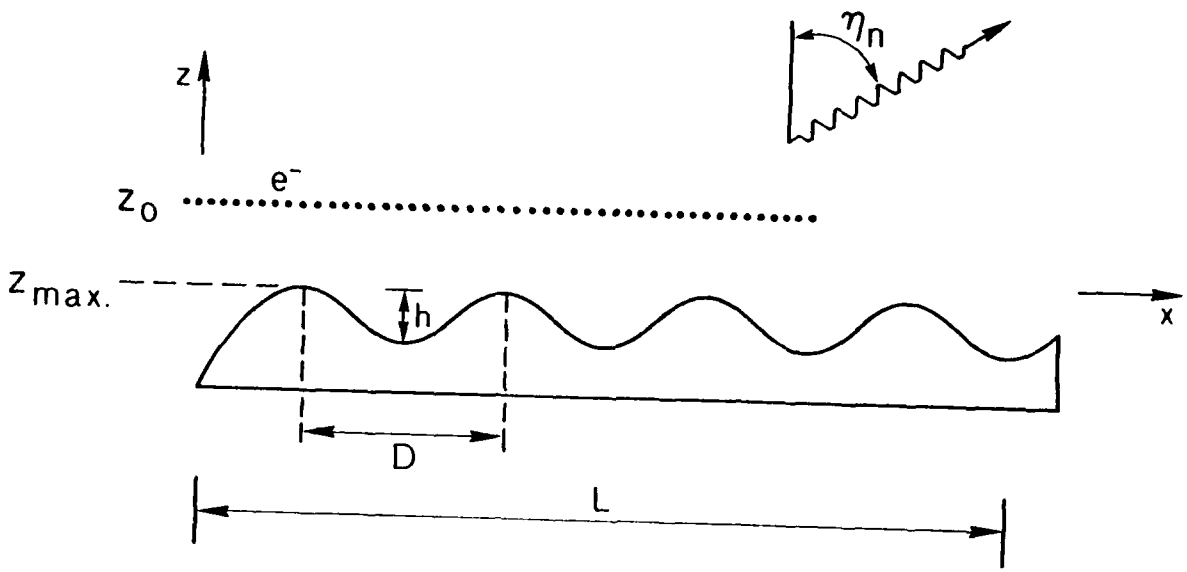


Fig. 1. Schematics of the Smith-Purcell radiation effect.

dispersion relation (1) in terms of a Huygens wave construction of the radiation emitted by the oscillating positive image charge of the electron inside the conductive grating[8]. Ishiguro and Tako used the oscillating dipole model to calculate the radiation power and radiation pattern using the known radiation formula of a moving dipole [9]. Their calculations did not fit very well with the measured Smith-Purcell radiation power and radiation pattern.

Since the image charge model requires the electrons to move very close to the grating (less than the grating period) only a small fraction of a finite cross section electron beam shot parallel to the grating will contribute significantly to the radiation. This motivated Salisbury to offer an alternative mechanism to explain the Smith-Purcell radiation effect[10]. According to Salisbury some of the electrons in the electron beam hit the grating surface at a shallow angle and are reflected by the tops of the rulings, forming current sheets with periodicity which is determined by the grating period. The space charge electric field which is associated with the reflected sheet current beamlets applies a periodic force on the other electrons across the incoming beam, and forces them to oscillate. Salisbury reported experimental results which were claimed to support his model. However no other independent study confirmed his result. Futhermore a complete quantitative calculation of the strength of Salisbury's mechanism was not given.

A useful model for solving the Smith-Purcell radiation problem was introduced by Toraldo di Francia who analized the radiation effect as a regular grating diffraction problem where the incoming wave is an

evanescent wave which appears when the moving electron point charge is expanded into its Fourier components[12]. This presentation of the Smith-Purcell radiation problem was further imporved by van-den-Berg[12] who rigorously solved the Maxwell equations with the optical grating boundaries (assuming ideal conductor sinusoidal grating). Matching boundary conditions at the electron beam coordinates resulted in an integral equation which was numerically solved and presented graphically in [12] for some exemplary parameters. van-den-Berg's analysis seems to be the most rigorous quantitative description of the Smith-Purcell radiation. However its quantitative predictions were not compared to experiments.

A number of experimental studies of the Smith-Purcell radiation effect were carried out since Smith and Purcell's experiment [13,14]. All of these studies confirmed the basic radiation condition (1). However little attempt was made to compare the quantitative power measurements to the predictions of the different theoretical models.

In the present report we base our experimental interpretation on van-den-Berg's model. The main features of the measured Smith-Purcell radiation pattern at various latitude and azimuth angles fit well with the theoretical curves derived from interpolation of van-den-Berg's example data.

In order to check Salisbury's model, we derive explicit expressions based on the known spontaneous emission formulas of free electron lasers to account for the radiation emission due to the space charge force radiation mechanism. It was found that the power emission predicted due to this mechanism is orders of magnitude lower than the power measured

experimentally. We conclude that Salisbury's model is irrelevant for the parameters of our experiment and probably all previous Smith-Purcell experiments.

The experimental results in agreement with van-den-Berg's model indicate stronger emission at azimuthal angles $\zeta$ off the plane which includes the electron beam line and is perpendicular to the grating. We point out the relevance of this observation to the resonator design for Smith-Purcell free electron lasers and orotrons.

## Theoretical Model

Our theoretical model is based on the theory of van-den-Berg[12]. The electro-magnetic radiation on top of the gratings (Fig. 1) is given in terms of a Floquet mode series

$$\underline{E}(\underline{r},t) = (2\pi^2)^{-1} \mathrm{Re} \int_0^\infty d\omega \int_{-\infty}^{\infty} dk_y \, \underline{\mathcal{E}}(x,y,k_y,\omega) \exp(ik_y y - i\omega t) \quad (2)$$

$$\underline{\mathcal{E}}(x,y,k_y,\omega) = \sum_{n=-\infty}^{\infty} \underline{\mathcal{E}}_n(k_y,\omega) \exp(ik_{xn}x + ik_{zn}z) \quad (3)$$

where

$$k_{xn} = k_{x0} + n\,2\pi/D$$
$$k_{zn} = (k^2 - k_y^2 - k_{xn}^2)^{1/2} \quad (4)$$

where $k = \omega/c$.

The zero order space harmonic (n=0) is chosen to be synchronous with the $\omega$ frequency Fourier component of the single electron current $-ev_0\,\delta(x-v_0t, y, z-z_0)i_x$:

$$\underline{J}(x,y,z,\omega) = - \qquad \exp(i\frac{\omega}{v_0}z)\,\delta(z-z_0)\,\hat{i}_x \quad (5)$$

so that $k_{xo}=\omega/v_o$. It follows from (4) that this space harmonic is necessarily nonradiating (evanescent in the z direction) since $k^2-k_y^2-(\omega/v_o)^2<0$. However some of the negative order space harmonics (diffraction orders) may be radiative if $k^2-k_y^2-k^2_{xn}>0$. The radiation directions can be defined in terms of the angular coordinate systems $(\eta_n,\zeta_n)$ which are illustrated in Fig. 2.

$$\begin{aligned} k_{xn} &= k \sin\eta_n \\ k_{yn} &= k \cos\eta_n \sin\zeta_n \\ k_{zn} &= k \cos\eta_n \cos\zeta_n \end{aligned} \tag{6}$$

The synchronization condition $\omega/v_o=k_{xo}$ together with Eqs. 4(a), 6(a) are sufficient to determine the radiation condition (1). Clearly, only negative diffraction orders $n<0$ can radiate. Radiation is possible at all wavelengths $\lambda$ and orders n which satisfy the inequality $|\sin\eta_n|=|c/v_o + n\,\lambda/D|<1$. The radiation wavelength $\lambda$ is only a function of the angle $\eta$ and is independent of $\zeta$. Consequently, the Smith-Purcell radiation appears as a rainbow of continuously varying colors (wavelengths), where each color is emitted along directions which define a half cone of half angle $\pi/2-\eta$ whose axis lies along the beam propagation direction.

While the radiation (dipersion) condition (1) was derived without complete solution of the electromagnetic radiation field, derivation of the absolute optical power emission and the angular radiation pattern required a detailed solution for the electromagnetic fields in the presence of the electron beam as was done in [12]. The translation symmetry in the y direction, which allowed us to define the radiation

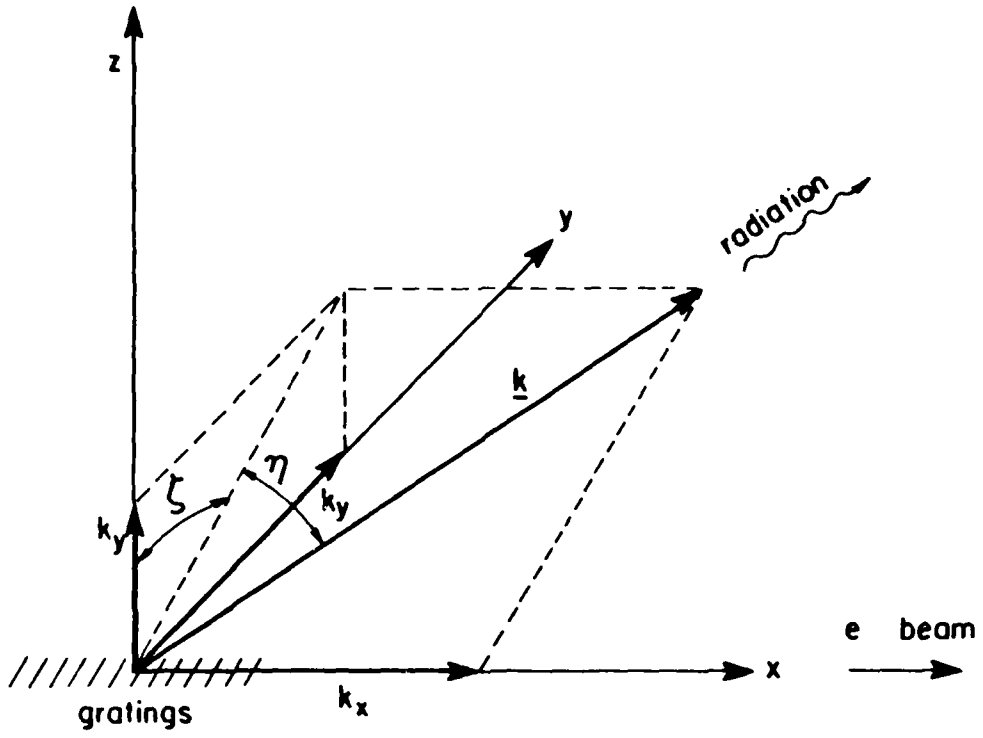


Fig. 2

Fig. 2. Definition of the latitude (2) and azimuth (η) angles of a Smith-Purcell diffraction order.

modes with a single wavenumber $k_y$, also permits separation into two different modes: the E polarization for which $\mathcal{E}_y \neq 0, \mathcal{H}_y = 0$ and the M polarization for which $\mathcal{E}_y = 0$ $\mathcal{H}_y \neq 0$. All of the field components of the E polarization can be presented in terms of $\mathcal{E}_{yn}$:

$$
\begin{aligned}
\mathcal{E}_{yn} &= \phi_n(k_y, \omega) \\
\mathcal{E}_{xn} &= -\frac{k_y k_{xn}}{k^2 - k_y^2}\,\phi_n \\
\mathcal{E}_{zn} &= -\frac{k_y k_{zn}}{k^2 - k_y^2}\,\phi_n \\
\mathcal{H}_{xn} &= -\sqrt{\frac{\epsilon_o}{\mu_o}}\,\frac{k k_{zn}}{k^2 - k_y^2}\,\phi_n \\
\mathcal{H}_{yn} &= 0 \\
\mathcal{H}_{zn} &= \sqrt{\frac{\epsilon_o}{\mu_o}}\,\frac{k k_{xn}}{k^2 - k_y^2}\,\phi_n
\end{aligned}
\tag{7}
$$

All the field components of the M polarization may be presented in terms of $\mathcal{H}_{yn}$:

$$
\begin{aligned}
\mathcal{H}_{yn} &= \Psi_n(k_y, \omega) \\
\mathcal{H}_{xn} &= -\frac{k_y k_{xn}}{k^2 - k_y^2}\,\Psi_n \\
\mathcal{H}_{zn} &= -\frac{k_y k_{zn}}{k^2 - k_y^2}\,\Psi_n \\
\mathcal{E}_{xn} &= \sqrt{\frac{\mu_o}{\epsilon_o}}\,\frac{k k_{zn}}{k^2 - k_y^2}\,\Psi_n \\
\mathcal{E}_{yn} &= 0 \\
\mathcal{E}_{zn} &= -\sqrt{\frac{\mu_o}{\epsilon_o}}\,\frac{k k_{xn}}{k^2 - k_y^2}\,\Psi_n
\end{aligned}
\tag{8}
$$

The Poynting vector power density of the n order <u>radiating</u> space harmonic is propagating in the direction of the $\underline{k}_n$ propagation vector and given by

$$
\frac{1}{2}\,\underline{\mathcal{E}}_n \times \underline{\mathcal{H}}_n^{*} = \frac{1}{2}\left(k^2 - k_y^2\right)^{-1} \omega \left(\epsilon_o \phi_n \phi_n^{*} + \mu_o \Psi_n \Psi_n^{*}\right) \underline{k}_n \tag{9}
$$

The energy which is lost by a single electron by radiation when traversing one period length D is found to be the sum of the Poynting

vector powers (9) in the z direction of all radiating space harmonics integrated over all $\omega$ and $k_z$ and multiplied by D: (10)

$$W = \frac{e^2}{D\varepsilon_0} \sum_{\substack{\text{radiating} \\ \text{waves } n}} \int_0^{\pi/2}\int^{\pi/2} \frac{\cos^2\eta\cos^2\xi}{(1/\beta_0 - \sin\eta)^3} \left|R_n(\xi,\eta)\right|^2 \exp\left[-\frac{z_0 - z_{max}}{h_{int,n}(\xi,\eta)}\right] \cos\eta\, d\eta\, d\xi$$

where (11)

$$h_{int_n} = \frac{D(\beta^{-1} - \sin\eta)}{4\pi n\left[\beta_0^{-2} - 1 + \cos^2\eta\sin^2\xi\right]^{1/2}} = \frac{\lambda_n}{4\pi\left[\beta_0^{-2} - 1 + \cos^2\eta\sin^2\xi\right]^{1/2}}$$

The parameter $|R_n(\xi,\eta)|^2$ can be calculated from $\phi_n, \psi_n$ after these functions are computed from the equations resulting by matching boundary conditions at the beam position $z=z_0$ and the grating surface. Assuming ideal conductor sinusoidal grating the parameter $R_{-1}(\xi,\eta)$ was numerically computed by van-den-Berg and was illustrated for various values of v/c and h/D[12].

The parameter $h_{int}(\xi,\eta)$ is the effective interaction length. Only electrons passing within the interaction length above the grating $z_0 - z_{max} < h_{int}(\xi,\eta)$ contribute effectively to the n-order Smith-Purcell radiation in the $(\xi,\eta)$ direction. For nonrelativistic or moderately relativistic electron beam $h_{int}$ is a fraction of a wavelength. Thus at the optical wavelength only a small portion of the electron beam current is effective in the interaction and the radiation is weak.

The integrand of Eq. 10 is the radiative energy emitted at direction $(\eta,\xi)$ per period length D per solid angle. Assuming that the electron beam fills up the region above $z=z_{max}$ and well above $z_{max}+h_{int}$ with uniform current density J, then the power emitted by the total beam at direction $\eta,\xi$ per unit solid angle is obtained by multiplying this integrand by the electrons flux density J/e, the e-beam width b and the number of periods in the gratings L/D, and then integrating over z from $z_{max}$ to infinity:

$$I_n(\zeta,\eta) = \frac{e J b L}{4\pi\epsilon_0 D n} \frac{\cos^2\eta \cos^2\zeta}{(\beta^{-1} - \sin\eta)^2 (\beta^{-2} - 1 + \cos^2\eta \sin^2\zeta)^{1/2}} |R_n(\zeta,\eta)|^2$$

Fig. 3 illustrates the theoretical angular power distribution $P_{det}(\zeta,\eta)=I_n(\zeta,\eta)\Omega_{det}$ which is expected to be collected by a detector placed at angle $(\zeta,\eta)$ according to van-den-Berg's theory and the assumed parameters of our experiment. The radiation factor $|R_{-1}(\zeta,\eta)|^2$ was calculated for the experiment parameters by interpolation of the parameter values given by van-den-Berg. The assumed expermental parameters of Fig. 3 are: $h/D=1/3$, $E=100$ keV ($\beta=0.55$), the solid angle intercepted by the detector was $\Omega_{det}=0.005$ ster, $J=0.8$ mA/cm$^2$, the beam width $b=0.2$mm, $1/d=3600$ lines/mm, $n=-1$, $L=2.5$cm.

Though Fig. 3 is based on a crude interpolation it is believed to reflect the gross features and the approximate quantitative values of the radiation pattern as predicted by van-den-Berg's theory. The minimum of the curves around $\eta=30°$ corresponds well with the Doppler shifted (relativistic transformation) node of a purely transversely oscillating moving dipole: $\eta_{min}$= arc sin $(\beta_o)=32°$. The curves also feature a maximum for the radiation pattern as a function of $\zeta$ which occur for each latitude angle $\eta$ at different azimutal angle $\zeta$, $0°<\zeta<90°$.

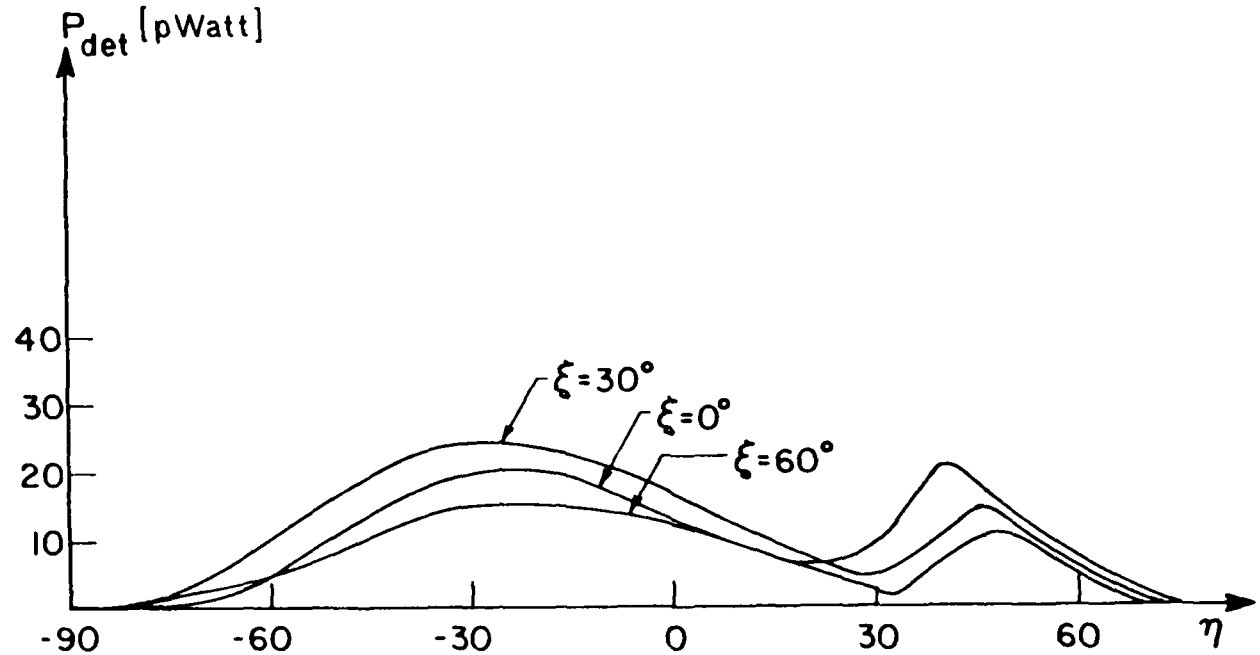


Fig. 3

Fig. 3. The Smith-Purcell radiation power detected by a detector as a function of $\eta$ for various azimuthangles $\zeta$ as calculated from van den Berg's graphs [12] for grating and beam parameters corresponding to the experiment.

Salisbury's Model

An alternative physical mechanism was suggested by Salisbury to explain the Smith-Purcell radiation[10]. According to Salisbury's model the electrons hit the grating at a small angle and are reflected at the top of the grating rulings, producing thin parallel sheet beamlets with a period along the x axis which is equal to the gratings period (see Fig. 4). According to Salisbury's model the periodic space charge field of these sheet beamlets operates as a wiggler on the incoming electrons in the beam. Though this possible mechanism should be weak because the space charge field of the beam is expected to be very small, it has the favorable feature that the interaction length limitation (11) is eliminated and the entire cross section of the beam is capable of participating in the interaction. Salisbury's model was not yet confirmed or discarded by an independent study. As we show here by careful computation of the effect predicted by Salisbury's model, this model is inappropriate for explaining the radiation power levels measured in our experiment, and probably other similar experiments.

The current density and space charge density modulation of the sheet current beamlets is taken to be $J_o \cos [2\pi x''/(D\sin\theta_i)]$ and $(J_o/v_o) \cos [2\pi x''/(D\sin\theta_i)]$ respectively where $x''$ is a coordinate perpendicular to the current sheets (see Fig. 4). The space charge field in the direction of the incoming e-beam and in the perpendicular direction, and the magnetic field are directly integrated from Maxwell equations

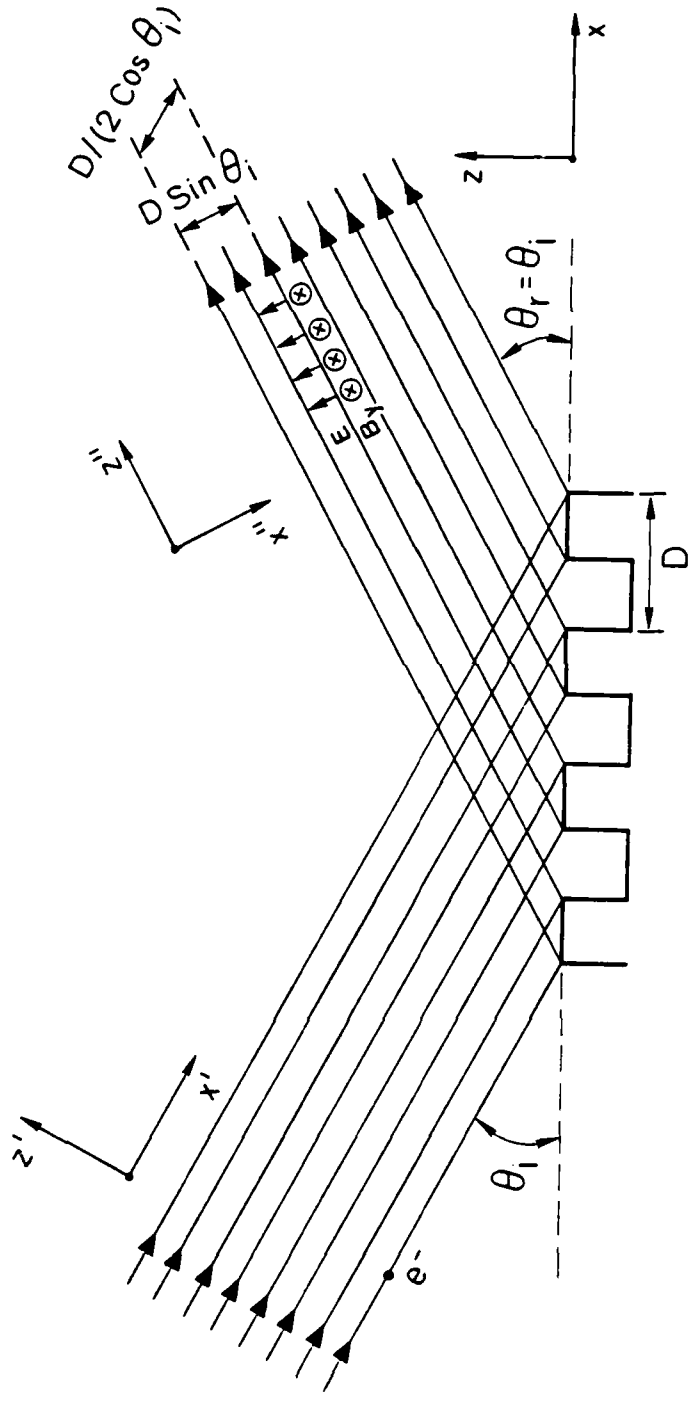


Fig. 4. The configuration of Salisbury's radiation mechanism.

$$E_{x'} = \frac{1}{2\pi}\sqrt{\frac{\mu_0}{\epsilon_0}}\frac{J_0}{\beta_0} D \sin(\theta_i)\sin(2\theta_i)\sin\left(\frac{4\pi\cos\theta_i}{D}x'\right) \tag{13}$$

$$E_{y'} = \frac{1}{2\pi}\sqrt{\frac{\mu_0}{\epsilon_0}}\frac{J_0}{\beta_0} D \sin(\theta_i)\cos(2\theta_i)\sin\left(\frac{4\pi\cos\theta_i}{D}x'\right) \tag{14}$$

$$B_{y'} = \frac{1}{2\pi c}\sqrt{\frac{\mu_0}{\epsilon_0}} J_0 D \sin(\theta_i)\sin\left(\frac{4\pi\cos\theta_i}{D}x'\right) \tag{15}$$

In the limit of grazing incidence ($\theta_i \ll \pi$) in which most Smith-Purcell experiments are conducted, the period of the wiggling forces which are experienced by the electrons is D/2. Consequently it turns out that the radiation orders (due to the periodic wiggler "synchrotron" radiation generated by the periodic forces) will coincide only with the even orders of the Smith-Purcell radiation given by (1). Thus radiation at the 1st order is not explained by this mechanism.

When $\theta_i \ll \pi$ the longitudinal electric field modulation $E_x$ diminishes relative to the transverse field $E_z$. Futhermore, for relativistic beams the transverse Lorentz force $ev_0B_y$, which was ignored by Salisbury altogether, is comparable to the transverse electric force $eE_z$ (reduced by a factor $\beta_0^2$). They both go to zero in proportion to $\theta_i$ when $\theta_i \ll \pi$.

The spontaneous emission theory of magnetic bremsstrahlung (synchrotron radiation) free electron lasers[15] can be straightforwardly adopted to describe the spontaneous emission due to the transverse wiggling force $e(E_x + v_0B_y)$. In terms of the angle coordinates $(\xi,\eta)$ the radiation pattern is given by (16)

$$I(\xi,\eta) = \frac{eI_0 a_w^2 k_w^2 L}{32\pi^2\epsilon_0\gamma_0^2\beta_0^2}\,\frac{\cos^2\xi(\beta^{-1}-\sin\eta)^2 + \sin^2\xi(\beta^{-1}\sin\eta - 1)^2}{(\beta^{-1}-\sin\eta)^5}$$

where

$$a_w = \frac{e}{k_w mc}\left(B_w + \frac{1}{v_0}E_w\right) = \frac{eDJ_0\sqrt{\mu_0/\epsilon_0}\sin\theta_i}{2\pi k_w mc^2}\left(1 + 1/\beta_0^2\right) \tag{17}$$

and $k_w = 4\pi/D$.

We calculated the power distribution $P_{det}(\zeta,\eta)=I(\zeta,\eta)\Omega_{det}$ which would be predicted by (15) using the same experimental parameters as before. The radiation pattern exhibits similar behavior to that predicted by van-den-Berg's model, including the dip at angle $\eta$=arc sin$\beta$=32°; however the absolute power emission is significantly smaller. Even for a large incidence angle $\theta_i$=1°, the power collected by the detector should be $5\times10^{-11}$ watts multiplied by the angular dependence factor of Eq. 16. This is much smaller than the power predicted in Fig. 3. It is also significantly smaller than the minimum power which can be detected by our detector.

Experimental Procedure and Results

We used a Philips EM300 Electron microscope to produce a 0.25μA, 200μm diameter circular e beam. The divergence of the beam was less than 1 m rad, and the beam voltage was 60, 80, or 100KeV ($\beta$=0.443, 0.503 and 0.550 responsively). The grating we used, was a 1"x1" aluminium coated replica grating with 1800 ruling lines per mm. The radiation was detected using a sensitive Hamamtsu R 936 photomultiplier.

The power detected was calibrated using the photomultiplier Response Curves and taking into consideration the window absorption.

The measured S.P. power in the -2 diffraction order is drawn in Fig. 5 versus angle $\zeta$ at 100 keV for $\eta$=0°, -16°, -23°. The variation of the measured power versus the angle $\eta$ at a fixed $\zeta$=37.5 is presented in Fig.6. We also measured S.P. power versus electron energy $\beta$ (for 60, 80 and 100 keV) and we found, in accordance with most existing theories for the S.P. effect, that the power increased very fast with increasing $\beta$. By going from $\beta$=0.443 to $\beta$=0.550 the power was tripled.

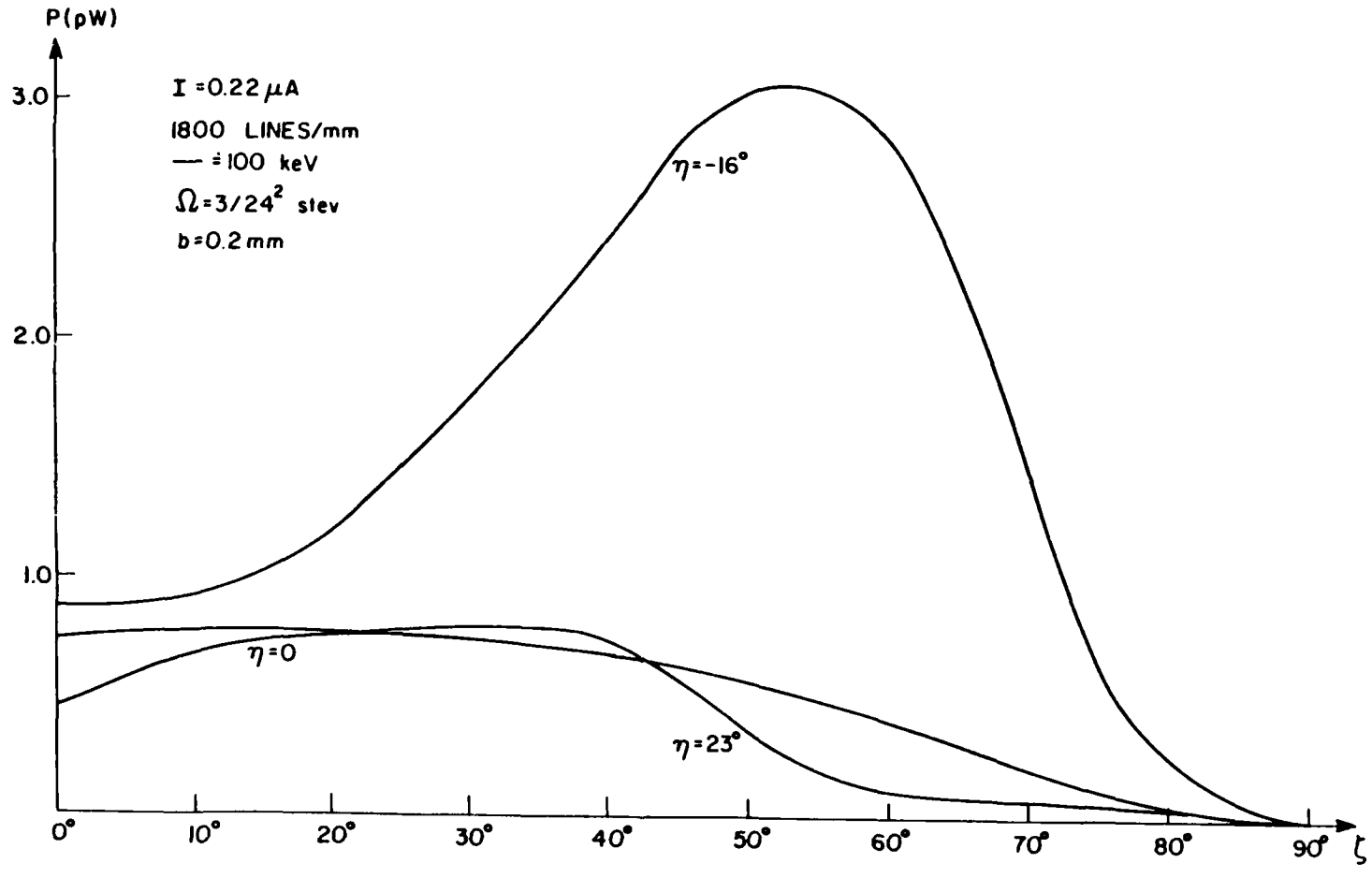


Fig 5

Fig. 5. Measured -2 order Smith-Purcell radiation power as a function of the azimuth angle $\zeta$.

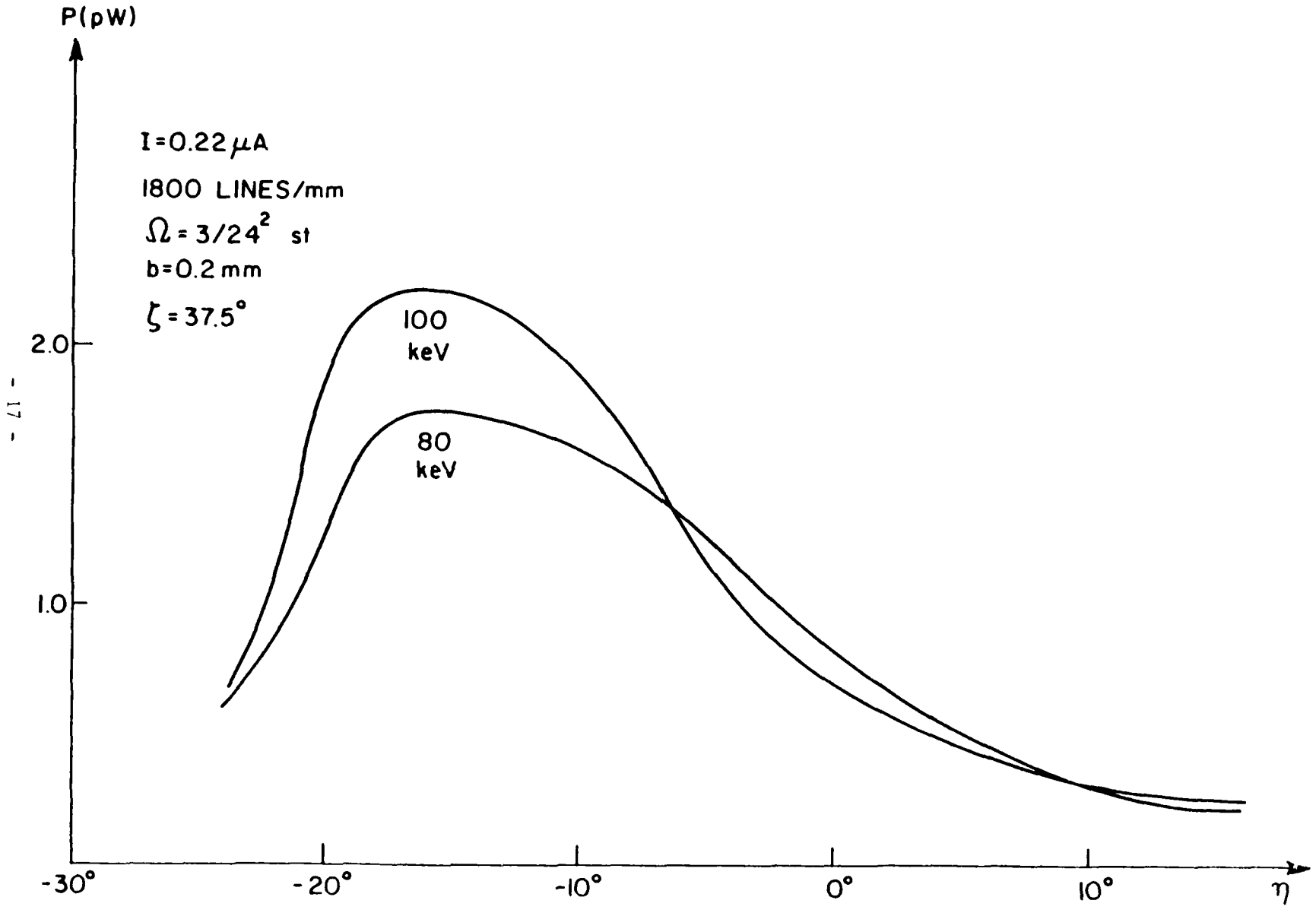


Fig. 6. Measures -2 order Smith-Purcell radiation power as a function of the latitude angle η.

Discussion

The main features of the radiation distribution which was measured as a function of $(\zeta,\eta)$ (Figs. 5,6) agree quite well with van-den-Berg's theoretical model for Smith-Purcell radiation (Fig. 3). The measured absolute power levels are about an order of magnitude lower than the theoretical prediction. Since van-den-Berg's analysis was made for -1 order diffraction from an ideal conductor sinusoidal gratings its application to our experiment for a blazed grating and -2 order diffraction should not give more than the main features of the radiation pattern and order of magnitude or upper limit values for the radiation power.

The experimental confirmation of the dispersion relation (1) was evident. We also verified that the radiation wavelength did not change as a function of $\zeta$ and was only dependent on $\eta$. Nevertheless this by itself is not a check for the validity of the theoretical model or even the physical mechanism. Toraldo di Francia's model would predict exactly the same dispersion realtion, but his prediction for the angular power distribution and power levels deviates substantially from the measured parameters. As we mentioned before confirmation of the dispersion relation (1) in the second order is also consistent with Salisbury's model, and so is the radiation pattern measured. However the absolute value of the radiation power due to Salisbury's model is so much smaller than the measured power, that it must be rejected as a possible explanation for our experiment or similar ones.

An important feature of the computed and measured radiation distribution curves is the fact that the radiated power peaks up at azimuthal angles $\zeta \neq 0$. This has substantial relevance to the design of Smith-Purcell free electron lasers since we expect that also the stimulated emission is increased at the radiation directions in which the spontaneous Smith-Purcell radiation is high[16]. Thus in an open resonator Smith-Purcell free electron laser it may be advantageous to build the resonator from 3 or 5 mirrors. One of them is the grating itself and the other placed at directions $(\pm\zeta_m, \pm\eta_m)$ where $\zeta_m$ is the angle at which the emission is maximal (see Fig. 7a). In milimeter wavelength Orotron devices [4-7] the resonator is made out of the grating and a convex mirror right above it $(\zeta=0, \eta=0)$. We suggest that also in this device it may be preferable to replace the convex mirror by two mirrors at angles $(\zeta=\pm\zeta_m, \eta=0)$.

In a Smith-Purcell FEL based on a rectangular waveguide it may be preferable to choose waveguide modes which have "zig-zag" bouncing angles close to $\zeta_m$ (see Fig. 7b). In the infrared regimes the waveguide modes are leaky modes whose losses are strongly dependent on the mode zig-zag angles. If the waveguide is largely over moded, the mode losses may be small enough to be used in a laser oscillator or amplifier configuration[17,18].

Rectangular waveguides seem to be most appropriate for Smith-Purcell FELs since they incorporate the gratings as one of the waveguide walls. The leaky modes of a rectangular metal-dielectric waveguide longitudinal section magnetic and longitudinal section electric are identical with the E type and H type modes given in (7), (8) except that the transverse

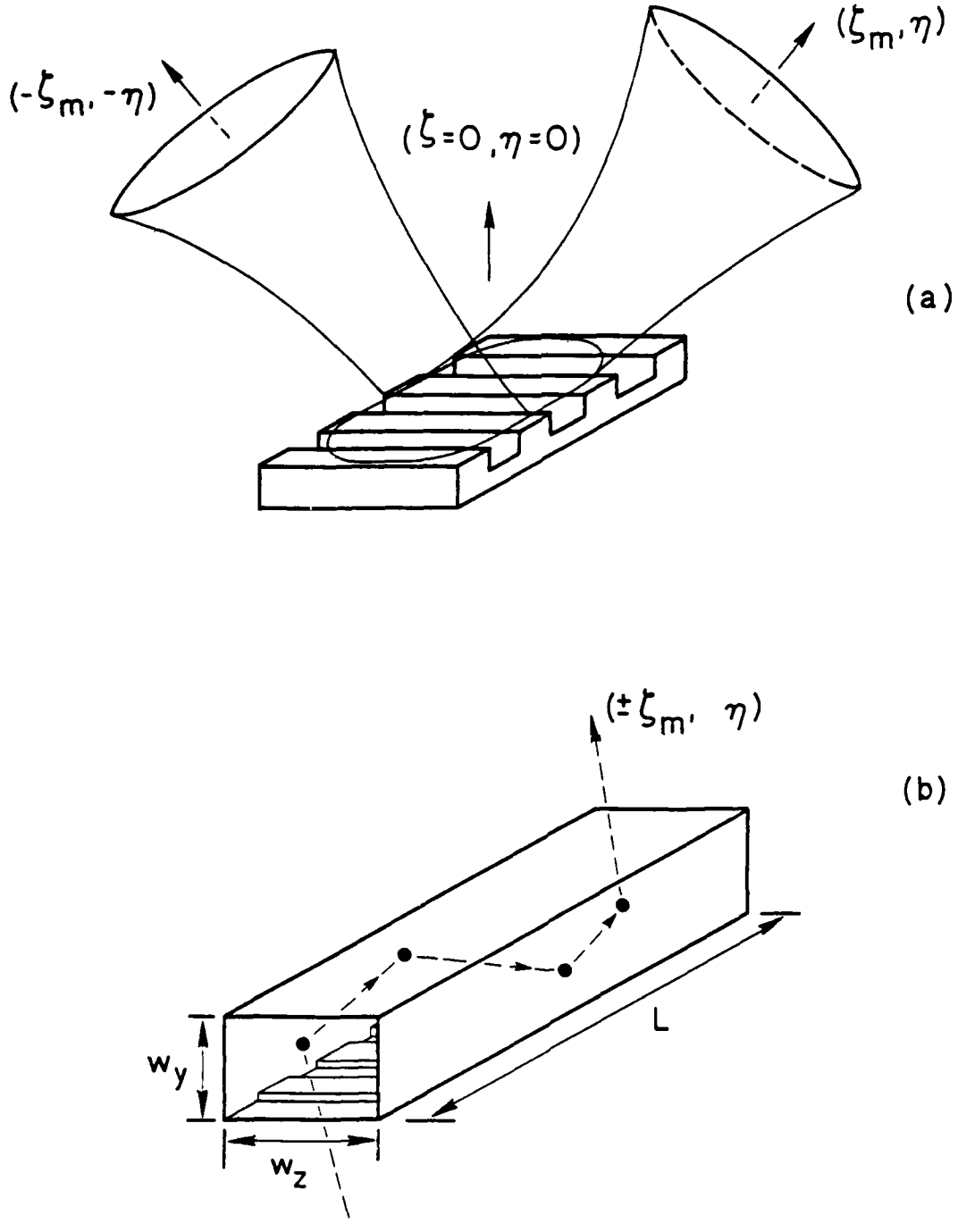


Fig. 7. Proposed optimal resonator configurations for Smith-Purcell FELs. (a) A 3 mirror open cavity resonator. (b) A rectangular waveguide or closed cavity resonator.

wave numbers $k_x$, $k_y$ are quantized by the finite dimensions of the guide cross section $k_y=p\pi/w_y$ $k_z=q\pi/w_z$. In a hollow rectangular waveguide the high order leaky eigenmodes are Hybrid modes E $H_{qp}$ [17]. The field attenuation constant of such modes is given by

$$\alpha_{pq} = \frac{2\pi^2}{k^2}\left[\frac{p^2}{w_y^3}\,Re\left(\frac{1}{\sqrt{\nu^2-1}}\right) + \frac{q^2}{w_z^2}\,Re\left(\frac{\nu^2}{\sqrt{\nu^2-1}}\right)\right] \qquad (18)$$

where $\nu$ is the complex index of refraction of the waveguide walls.

For a high order mode in an over moded waveguide we may substitute $p=k_y w_y/\pi$ $q=k_z w_z/\pi$ and use Eq. (6). Hence

$$\alpha_{pq} = 2\cos^2\eta\left[\frac{\sin^2\zeta}{w_y}\,Re\left(\frac{1}{\sqrt{\nu^2-1}}\right) + \frac{\cos^2\zeta}{w_z}\,Re\left(\frac{\nu^2}{\sqrt{\nu^2-1}}\right)\right] \qquad (19)$$

For a given operating wavelength, $\lambda$, diffraction order n and beam velocity $v_o$, $\eta$ is uniquely determined by the dispersion relation (1). The freedom to choose $\zeta$, $w_y$, $w_z$ allows for the designing of an FEL cavity with low mode attenuation. Generally $Re\left(\nu^2/\sqrt{\nu^2-1}\right) > Re\left(1/\sqrt{\nu^2-1}\right)$

For this reason it is preferable to choose $\zeta$ large in order to keep the second term in (19) small. This is favorably consistent with the fact that stronger emission is also expected at a higher value of $\zeta$. In a Smith-Purcell FEL design it is expected that the zig-zag angle will be chosen near the maximum emission angle $\zeta=\zeta_m$. The choice of waveguide cross section dimensions gives then a degree of freedom for minimizing waveguide attenuation of the preferable mode.

We would like to acknowledge the valuable technical assistance of T. van der Hagen and H. Kleinman and useful communications with G. Hughes and J. P. Bachheimer.

REFERENCES


1. A. Gover and A. Yariv, Physics of Quantum Electronics, Vol. 5, p. 197, S. Jacobs, M. Sargent III, M. Scully Eds., Addison Wessley Pub. (1977).

2. A. Gover and Z. Livni, Optics Communications 26, 375 (1978).

3. J. Wachtel, J. Appl. Phys. 50, 49 (1979).

4. F. S. Rusin and G. D. Bogomolov, Proc. IEEE 57, 720 (1969).

5. V. K. Korneyekov and V. P. Shestopolov, Soviet Radio eng. Elect. Phys. 22, 148 (1977).

6. K. Mizuno, S. Ono and Y. Shibata, IEEE Transac. ED-20, 749 (1973).

7. R. P. Levitt, D. E. Wortman and H. Dropkin, IEEE J. QE-17, 1333, 1341 (1981).

8. S. J. Smith and E. M. Purcell, Phys. Rev. 92, 1069 (1953).

9. K. Ishiguro and T. Tako, Opt. Acta 8, 25 (1961).

10. W. W. Salisbury, J. Opt. Soc. Am. 60, 1279 (1970).

11. G. Toraldo di Francia, Nuovo Cimento, 16, 61 (1960).

12. P. M. Van Den Berg, J. Opt. Soc. Am. 63, 1588 (1973).

13. J. P. Bachheimer, Phys. Rev. B 6, 2985 (1972).

14. E. L. Burdette and G. Hughes, Phys. Rev. A 14, 1766 (1976).

15. A. Gover, H. Freund, V. L. Granatstein, J. H. McAdoo and C. M. Tang, to be published in Ifrared and Millimeter Waves Vol 12: Millimeter Component and Techniques, Part III, K. J. Button Editor, Academic Press, 1983.

16. J. M. J. Madey, IL Nuovo Cimento 50 B, 65 (1979).

17. B. Adam, F. Kneubuhl, Appl. Phys. 8, 281 (1975).

18. A. Gover and P. Dvorkis, Tel Aviv Univ. School of Engin. Quantum Elect. Lab. AFOSR-77-3445 progress report (Oct. 78 - Sept. 79).

## Figure Captions

Fig. 1. Schematics of the Smith-Purcell radiation effect.

Fig. 2. Definition of the latitude ($\eta$) and azimuth ($\zeta$) angles of a Smith-Purcell diffraction order.

Fig. 3. The Smith-Purcell radiation power detected by a detector as a function of $\eta$ for various azimuth angles $\zeta$ as calculated from van-den-Berg's graphs for grating and beam parameters corresponding to the experiment.

Fig. 4. The configuration of Salisbury's radiation mechanism.

Fig. 5. Measured -2 order Smith-Purcell radiation power as a function of the azimuth angle $\zeta$.

Fig. 6. Measured -2 order Smith-Purcell radiation power as a function of the latitude angle $\eta$.

Fig. 7. Proposed optimal resonator configurations for Smith-Purcell FELs. (a) A 3 mirror open cavity resonator. (b) a rectangular waveguide or closed cavity resonator.

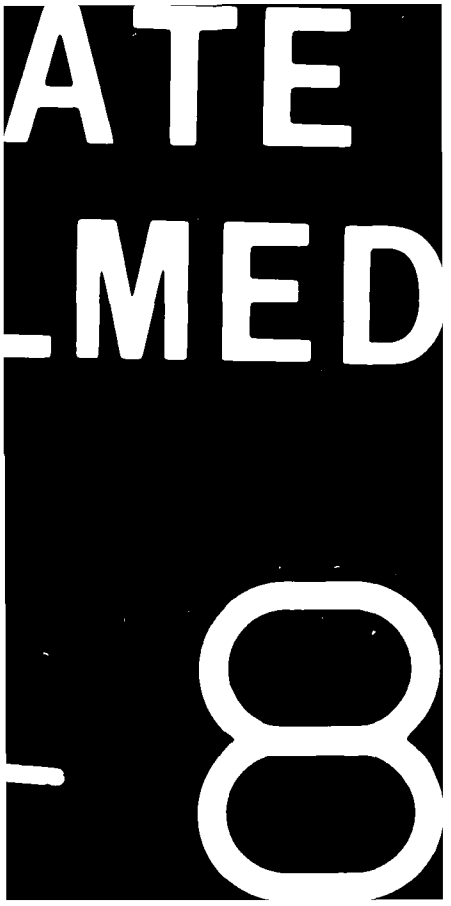
ATE
LMED
8